

Low-cost portable potentiostat for real-time insulin concentration estimation based on electrochemical sensors

Fitria Yunita Dewi¹, Harry Kusuma Aliwarga², Djati Handoko¹

¹Department of Physics, Faculty of Mathematics and Natural Sciences, Universitas Indonesia, Depok, Indonesia

²UMG IdeaLab, Jakarta, Indonesia

Article Info

Article history:

Received Jun 11, 2024

Revised Mar 19, 2025

Accepted May 23, 2025

Keywords:

Cyclic voltammetry

Electroactive surface area

Insulin detection

Multiple predictors

Portable potentiostat

Real-time detection

ABSTRACT

Administering incorrect insulin dosages to diabetic patients can be fatal, leading to severe health consequences. Insulin detection, in conjunction with blood glucose monitoring, can significantly enhance diagnostic accuracy. Electrochemical methods for insulin detection offer a low-cost and portable solution. This study presents an insulin concentration estimation system using a customized electrochemical potentiostat operating in real-time via Bluetooth low energy (BLE). Conventional electrochemical sensing, which relies on calibration curves to determine concentration, poses accuracy limitations in portable devices. To address this, we implement a multiple-predictor approach that incorporates peak currents from multiple cycles of cyclic voltammetry responses and the electroactive surface area of a multi-walled carbon nanotube (MWCNT-COOH) modified screen-printed sensor. This modified sensor enhances sensitivity compared to bare screen-printed carbon sensors, making it suitable for low-volume and portable applications. Through cross-validation, our method demonstrated strong performance, achieving a determination coefficient (R^2) greater than 0.90 for all training dataset combinations and greater than 0.85 for all testing dataset combinations. Hypothesis testing further confirmed the statistical significance of the electroactive surface area ($p=0.006$) as predictor, indicating its meaningful contribution to concentration estimation. This approach improves portable detection performance, supporting the development of affordable and reliable personal insulin monitoring systems.

This is an open access article under the [CC BY-SA](https://creativecommons.org/licenses/by-sa/4.0/) license.



Corresponding Author:

Djati Handoko

Department of Physics, Faculty of Mathematics and Natural Sciences, Universitas Indonesia

Depok, Indonesia

Email: djati.handoko@ui.ac.id

1. INTRODUCTION

Insulin regulates blood glucose levels in the body. This hormone is a polypeptide secreted by the pancreas and consists of 21 amino acids in the A chain and 30 amino acids in the B chain [1]. Dysfunction of this hormone secretion can cause diabetes which is one of the most common noncommunicable diseases [2]. According to the International Diabetes Federation (IDF), an estimated 537 million people are affected by diabetes, which is projected to reach 643 million by 2030 and 783 million by 2045 [3]. Diabetes current treatment involves insulin dosing [4], and proper adjustments can prevent the risks of hypoglycemia and hyperglycemia-related complications [5]. Blood glucose levels can help estimate the amount of insulin required, but because exercise and diet can affect blood glucose levels, a more accurate diagnosis can be achieved with the addition of insulin detection [6], [7].

Analytical methods for insulin detection can be developed using immunoassays, chromatography, and optical techniques. These methods are very time-consuming, slow, and high-cost, and require the modification of insulin molecules with isotopic or fluorogenic labels [8]. Therefore, electrochemical methods commonly associated with inexpensive and small instruments, fast responses, and simple preparation [4] are more suitable for point-of-care testing (POCT). The electrochemical approach can be utilized because insulin contains amino acids, such as tyrosine, tryptophan, and cystine, which are electroactive species [7].

Several electrochemical techniques can be employed for insulin detection. For example, cyclic voltammetry (CV) technique where the voltage applied to the electrodes is linearly increased and then decreased back to the initial voltage. The current response from CV contains information about oxidation/reduction reactions occurring in the analyte. In several studies, it has been observed that an increase in CV peak current is related to insulin concentration variations [1], [8]–[10]. The fitting between these peaks and concentration forms a calibration curve, with the slope indicating the sensitivity of the measurement. Determining concentration through a calibration curve is simple and straightforward. However, this calibration curve is specific to a particular sensor and cannot be applied to other sensors with different sensitivities. Even the same sensor can produce different calibration slopes due to the degradation of the sensor's performance over time and with repeated cycles. Therefore, in this study, the concentration estimation system is improved using a multiple predictors approach. While the calibration curve method relies on a single predictor, specifically the peak current, the proposed method incorporates multiple predictors, involving the sensor's performance information, to improve the accuracy of concentration estimation.

An instrument used to perform electrochemical techniques is commonly called a potentiostat. Commercially available potentiostats (benchtop instruments) provide a high resolution and can measure low currents with high precision and minimal noise. However, these potentiostats are expensive, large, heavy, and unsuitable for POCT applications [11], [12]. Although powerful for a wide range of applications, benchtop potentiostats are less suitable in resource-limited conditions, thus using customized, low-cost, and wireless potentiostats is more necessary.

The development of low-cost, portable potentiostats has surged recently, particularly open-source designs [12]–[16], which facilitate easy replication and allow the researchers to modify for specific analysis techniques and target analytes without starting from scratch. Bluetooth low-energy (BLE) selected as a connectivity option, is an interesting approach that allows for portable and low-power devices that can be easily implemented in mobile devices (smartphones and tablets). Several studies using Bluetooth and mobile device user interfaces have chosen different types of microcontroller units, such as board ESP32 in eSTAT [17], Arduino Nano in Paqaristat [18], BLE chipset in KAUSTat [11], RFDuino in UWED [12], and CC2541 in BluChem [19]. Their designs succeeded in building customized potentiostats at affordable prices (<\$100).

Most low-cost and portable potentiostats have been validated using the ferricyanide/ferrocyanide redox couple $[Fe(CN)_6]^{3-/4-}$ as a standard solution, and their performance has been evaluated through cyclic voltammetry at various concentrations or scan rates. However, very few studies have reported evaluations on specific analytes, as most devices have been developed for general electrochemical purposes [11], [12], [17], [20], [21] where the analyte responses fall within the device's current reading range. In this study, a low-cost and portable potentiostat specialized for insulin detection was designed. The estimation of the insulin concentration was then improved by incorporating information about the electrode surface area of the electrochemical sensor used. One advantage of developing customized potentiostat for insulin detection along with multi-predictors approach is to generally estimate concentration with different sensor's performance in real-time which is not possible with the use of benchtop potentiostat and a simple calibration curve (single-predictor approach).

2. METHOD

2.1. Sample preparation

Trisodium citrate ($Na_3C_6H_5O_7$), monopotassium phosphate (KH_2PO_4), and dipotassium phosphate (K_2HPO_4) were purchased from Merck, Singapore. 100 mL phosphate buffered saline (PBS) solution (0.1 M and pH 7) was prepared by dissolving 0.339 grams KH_2PO_4 and 2.022 grams K_2HPO_4 in distilled water. PBS was chosen as the solvent because it mimics physiological conditions, maintaining a stable pH to prevent structural changes in insulin, which is pH-sensitive. This ensures consistency in electrochemical measurements and minimizes variability in sensor responses.

Potassium ferricyanide $K_3[Fe(CN)_6]$, isopropanol, sodium hydroxide ($NaOH$) and sulfuric acid (H_2SO_4) were purchased from Smart Lab. Potassium ferricyanide was chosen as a redox probe. This redox probe was prepared by dissolving 0.33 grams of potassium ferricyanide in 50 mL PBS to achieve a final concentration of 20 mM.

Standard stock solutions of insulin were prepared by diluting 60 insulin units (IU) in 25 ml PBS solution i.e. $7.20 \mu\text{mol/L}$ ($1 \mu\text{IU/mL}$ equals to 6.0 pmol/L according to the American Diabetes Association conversion [22]). Concentration variations were prepared by diluting the stock to specified concentrations in PBS solution. These solutions may degrade over time due to adsorption onto container surfaces, particle contamination after long exposure to the surrounding air, and potential oxidation. Therefore, testing should be conducted immediately after sample preparation and within three days to ensure reliability. Extended storage might cause fine clumps of aggregation in the sample.

2.2. Apparatus

2.2.1. Sensor

Screen-printed carbon electrodes (SPCE) modified with carboxyl functionalized multiwalled carbon nanotubes (MWCNT-COOH) purchased from Metrohm DropSens were used as sensors. This type of SPCE (Ref. 110CNT DropSens) is a three-electrode system consisting of a surface-modified working electrode, carbon counter electrode, and silver reference electrode. Compared with the bare carbon electrode, the SPCE modified with MWCNT is expected to provide greater sensitivity and a broader linear range. This can be achieved owing to the capability of CNT to increase the surface area [4], decrease the overpotential of insulin [7], and minimize surface fouling [23]. The use of screen-printed electrode also tackles the problems arising from conventional electrodes, such as the necessity for a large amount of analyte for sensing analysis, difficulty in the cleaning process and modification of the larger electrode area [24].

2.2.2. Benchtop potentiostat

Electrochemical techniques were conducted using a Corrtest Instruments benchtop potentiostat (CS310M model). This instrument supports scan rates from 0.001 mV/s to $10,000 \text{ V/s}$, with a minimum potential gain of 0.075 mV , a voltage range of $\pm 10 \text{ V}$, a voltage resolution of $10 \mu\text{V}$, and a current resolution of 1 pA . Measurements involved connecting the SPCE to the potentiostat via a DropSens connector from Metrohm. All analyses used cyclic voltammetry, with parameters determined by sweeping specific voltage ranges over the insulin sample and identifying the reaction peak. The voltage and current response ranges from these measurements determine the design of the proposed potentiostat. Previous studies [4], [25], [26] have shown a distinct oxidation peak of insulin around 0.7 V in cyclic voltammetry, with peak shifts influenced by material modification, sample concentration, and external conditions (pH and temperature).

2.3. Hardware design

The general block diagram of the proposed device can be seen in Figure 1. This design was inspired by eSTAT, the low-cost portable potentiostat developed in [17]. While their work was intended to introduce basic electrochemistry for general purposes, this work was aimed for specific insulin detection. Therefore, the current reading range and its resolution was customized according to the prepared insulin concentration variations. The details of each block are as follows.

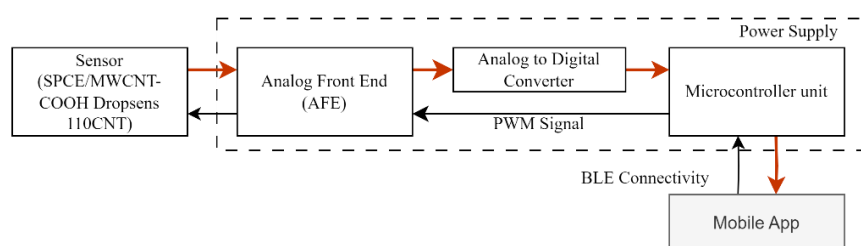


Figure 1. General block diagram of the proposed device

2.3.1. Microcontroller

The ESP32 development Board DevKit V1 was used as the microcontroller part of the design. The board is already equipped with an ESP-WROOM-32 module with Bluetooth, Bluetooth low energy (BLE) and Wi-Fi on a single chip, built-in voltage regulator and micro-USB port which are useful for the proposed design. This board is also compatible with boards and libraries management in the Arduino IDE software.

2.3.2. Analog/Digital converter

The ESP32 features a built-in 12-bit analog-to-digital converter (ADC) and an 8-bit digital-to-analog converter (DAC). For precise A/D conversion, especially for small currents, an external 16-bit

ADS1115 ADC was used with a programmable gain amplifier capable of boosting signals up to 16 times. This ADC offers a resolution as low as 0.125 mV within a 0-4.096 V range. The ESP32's 8-bit DAC resolution and signal-to-noise ratio are insufficient; therefore, pulse width modulation (PWM) is chosen for a compact and cost-effective design. The PWM signal is converted to a constant signal by a low-pass filter, achieving a DAC resolution that can exceed 8 bits depending on the PWM frequency configuration.

2.3.3. Analog circuit

Two key elements in a potentiostat are the control amplifier and the transimpedance amplifier (TIA). The control amplifier sets the electrode potential, whereas the TIA reads the current response and converts it to voltage. Additional components include level shifters, a buffer, and low pass filters. Two level shifters map the ESP32 voltage range (0 to 3.3 V) to the desired range (-1.5 to 1.5 V) and adjust the current reading voltage to the ADC working range (± 4.096 V). A buffer bridges the TIA and shifter for maintaining the converted voltage. One low-pass filter converts the ESP32 PWM signal into a DC signal, and another filters high-frequency noise before the ADC reads the signal. The TL084 op-amps which have 4 channels, low input bias current (30 pA at room temperature), low input offset voltage (3 mV at room temperature), and high slew rate (20 V/ μ s) is chosen as amplifiers. The schematic of the analog part is shown in Figure 2.

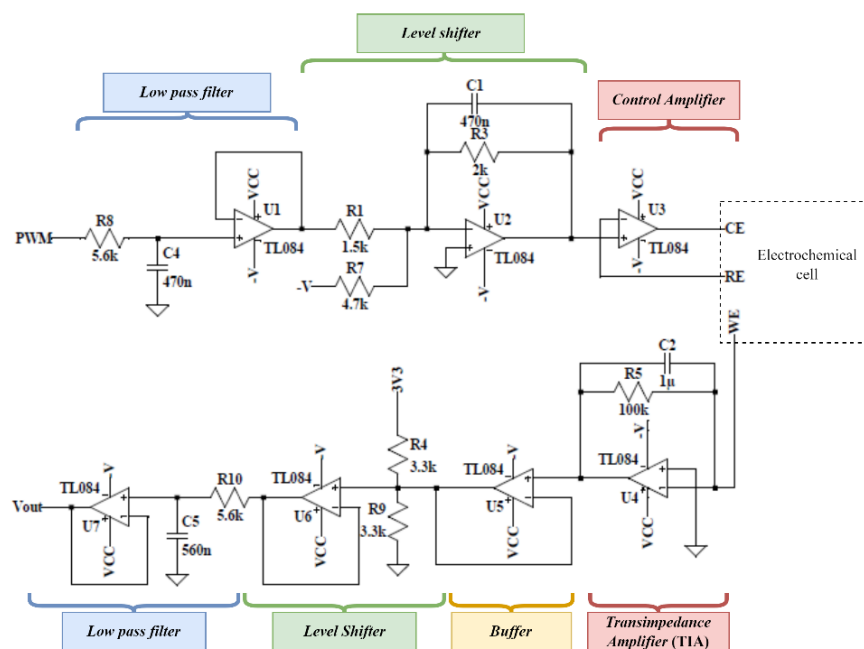


Figure 2. Schematic of the potentiostat's analog circuit

2.3.4. Power supply

The power for all components can be provided from a power bank or 18650 Li-ion battery accompanied by an 18650-shield connected via a micro-USB port on board and then regulated with the board's built-in 3.3 V power regulator. The negative voltage for operational amplifier is supplied by inverted voltage from ICL7660. Another negative voltage is supplied from LM2662 to provide more stable voltage. LM2662 has lower output impedance and higher output current than ICL7660 resulting in less voltage drop.

2.4. Estimation system

In this work, cyclic voltammetry analysis was used in determination of insulin concentration. Several studies showed that there is an apparent positive correlation between oxidation peak current in CV responses and concentration of insulin [4], [25], [26]. The calibration curve obtained between the peak current value and concentration is commonly used to characterize sensor performance in terms of sensitivity and to determine the voltage value for chronoamperometry analysis. Higher sensitivity can be due to larger electroactive surface area, because more active sites for reaction can lead to a higher current response. Therefore, information regarding the electroactive area of the sensor was included with the expectation that this approach will be applicable to various sensors with different sensitivities.

To calculate the electroactive area, several CVs were conducted in 20 mM $K_3[Fe(CN)_6]$ solution with various scan-rate and fit the linear regression of the peak current versus the square root of scan rate according to the Randles-Sevcik equation [27] given in (1).

$$i_p = 0.4463 \left(\frac{n^3 F^3}{RT} \right)^{\frac{1}{2}} AC^0 (D_0 v)^{1/2} \quad (1)$$

where i_p is the measured peak current in voltammogram (A), n is the number of electrons transferred in the reaction, F is Faraday's constant (96485 C/mol), C is the molar concentration of the redox species (20 mM), D is the diffusion coefficient of the redox species (± 7.3 cm²/s), R is the gas constant (8.3144 J/mol·K), T is the temperature (K), v is the scan rate (V/s) and A is the electroactive surface area (cm²).

Once the electroactive area of each sensor was calculated, CV data can be collected. CV measurements were carried out for each concentration by subtracting the peak responses from the baseline curve (response from a PBS sample in the absence of insulin). Each concentration experiment and its baseline were conducted using the same CV parameters, with voltage sweep from 0 to 0.8 V at a scan rate of 100 mV/s. Before each cycle, the sensor was cleaned and activated through pretreatment, as described in [1], where five cycles of CV were performed, sweeping from -0.2 to 1.1 V in alkaline NaOH solution. All CV measurements were collected using individual screen-printed sensors with either a benchtop potentiostat or our customized potentiostat to build different datasets. The estimation system, developed by training these datasets, is further explained in supplementary information section 4.

2.5. Implementation system

Our mobile application, developed on the MIT App Inventor platform, facilitates user-defined CV parameters such as scan rate, cycle number, and voltage range to be sent to the microcontroller via Bluetooth low energy (BLE). Sensor responses are transmitted to the application to be stored locally and forwarded to a server for processing concentration estimation. The process in the server is encapsulated in an API implemented with Flask framework which is accessible via HTTP. The mobile application can send CV responses by making a POST request while connected to the network. The server responds with the estimated concentration in JSON format that can be displayed in the app.

3. RESULTS AND DISCUSSION

3.1. Cyclic voltammetry analysis from benchtop potentiostat

From previous reports [4], [25], [26], CV responses of insulin indicate an irreversible reaction, as there is an apparent oxidation peak without a reduction peak. This reaction implies that successive scans result in a decreasing response current, as the material for the next reaction may be depleted. In Figure 3, the response of the subsequent scan with pretreatment using an alkaline solution remains quite stable and does not significantly decrease, whereas there is a reduction in response when no pretreatment is performed.

Three cycles of CV ranging from 0 to 0.8 V for each variation of insulin concentration measurement were performed. The resulting voltammogram for the first cycles at several concentrations is shown in Figure 4(a), and the calibration curve for each cycle is displayed in Figure 4(b). The peaks fitted in Figure 4(b) were obtained by subtracting the baseline curve (PBS with the absence of insulin), thereby isolating the peaks attributable solely to the Faradaic reaction.

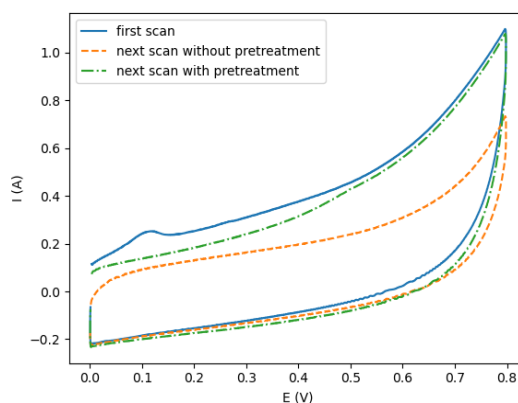


Figure 3. CV response of PBS with and without pretreatment

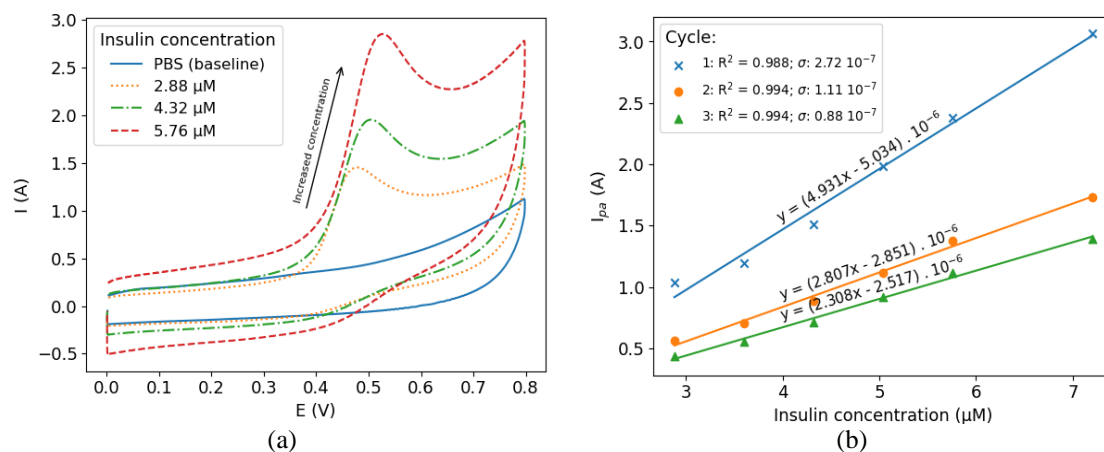


Figure 4. Peak current responses from various concentrations (a) at first cycle, and (b) all three cycles after subtracted from baseline current in the form of curve calibration

The fitting curve of the first cycle had the highest slope, indicating good sensitivity; however, it also had the highest standard error. Calculating electroactive area of each sensor also yielded different result depending on the sensor performance. The sensitivities for each cycle in each sensor, obtained by averaging three measurements, along with their corresponding electroactive areas, is listed in Table 1. Estimating concentration based solely on peak current will be unreliable due to variations in slopes among different sensors. Therefore, the aim in this study is to estimate concentration by incorporating information about the electroactive area, as the slope depends on it.

The performance comparison of fitting the regression with different selections of variables as predictors can be seen in Table 2. The variables involved are the peak currents from the first, second, and third cycles, abbreviated as I1, I2, I3 respectively, and the electrode's electroactive area. The data used for fitting were collected from measurements taken from 4 different sensors. The low R^2 value when using peak current from only one cycle as a predictor suggests that variations in concentration are inadequately explained by this predictor alone, especially given that peak currents differ across sensors. Incorporating peak current values from additional cycles and electroactive area significantly enhances R^2 , indicating that these new variables contribute to explaining concentration variations more effectively.

Table 1. Sensitivity from each cycle and the corresponding electroactive surface area for each sensor

Sensor number	Sensitivity ($10^{-1} \mu\text{A}/\mu\text{M}$)			Electroactive area (cm^2)
	Cycle #1	Cycle #2	Cycle #3	
1	5.97	3.89	2.78	0.0284
2	3.16	2.50	2.08	0.0257
3	7.53	4.31	3.65	0.0222
4	2.39	1.38	1.08	0.0128

Table 2. Comparison of regression fitting performance across various selected predictors

Predictor selection	R^2	MSE	MAE
I1	0.70	0.46	0.48
I2	0.79	0.35	0.40
I3	0.74	0.42	0.45
I2, A	0.81	0.32	0.42
I1, I2, A	0.84	0.28	0.37
I2, I3, A	0.92	0.15	0.30
I1, I2, I3, A	0.92	0.15	0.30

3.2. Hardware design

The analog part of our portable potentiostat was initially simulated using LTspice. Subsequently, the printed circuit board (PCB) layout was created using EasyEDA Designer. Finally, all components were soldered onto the PCB along with microcontroller, ADC, and supply regulator circuit. The final assembled form can be seen in Figure 5. The details of the PCB layout can be seen in the supplementary information section 2.



Figure 5. Assembled form of our potentiostat

3.2.1. Voltage output conversion

The process to generate the potential between electrodes for CV analysis involves several steps. First, the ESP32 generates a PWM signal with a frequency of 50 kHz. This signal is then filtered by a simple first-order low-pass filter consisting of a 5.6 k Ω resistor and a 470 nF capacitor, resulting in an approximately 60.47 Hz cutoff frequency. The next step involves mapping the filtered signal range from 0 to 3.3 V to the desired range. Figure 6 shows the plot of the resulting WE-RE potential with the corresponding 10-bit PWM digital values. Beyond 850 PWM digital value, the voltage increase saturates because the op-amp output voltage cannot fully reach its supply voltage. Therefore, to maintain linearity, this value was not exceeded and the final output range became -2 to 1.5 V, with 4.4 mV resolution and a very high R^2 value. This high value indicates that the voltage generated at the sensor will be highly linear with the PWM signal, which is controlled by the voltage parameter set by the user through the app interface.

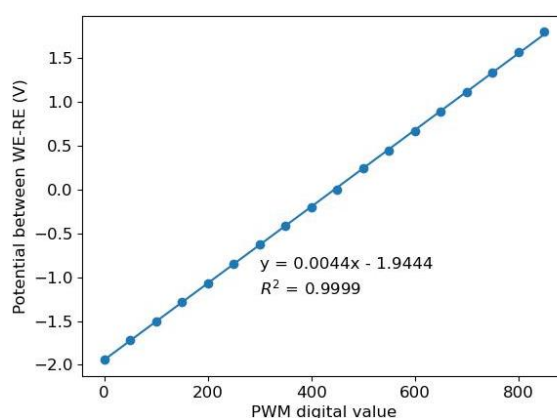


Figure 6. The generated WE-RE potential with corresponding PWM value

3.2.2. Current input conversion

ADS1115 can only read voltage, so the current from the sensor is converted to voltage by a transimpedance amplifier (TIA). To capture small currents in the order of several microamperes, a high resistor value for gain, specifically 200 k Ω , was used in our potentiostat. The resulting negative-to-positive voltage is then shifted using another level shifter to ensure the voltage falls within a positive range readable by the ADC. As depicted in Figure 2, there is an additional buffer which serves as a bridge between the TIA and the level shifter, ensuring that the voltage from the TIA remains unaffected by the level shifter's circuit. Additionally, a low-pass filter was added before the ADC reading to attenuate unwanted noise.

The ADC voltage must be calculated back into current units to obtain the I-V curve. Voltage scanning across test resistors allowed us to derive the conversion equation. According to Ohm's law, the current through a resistor is equal to the voltage across it divided by its resistance. By fitting the ADC readings to calculated currents, the average of slopes and biases for different resistors are obtained. We can use the averaged values since the variations in slope and bias across different resistors and scan rates were small and can be neglected. These values were then used to get the conversion formula below:

$$\text{Estimated current } (\mu\text{A}) = \text{average slope} \times \text{ADC voltage reading } (V) + \text{average bias} \quad (2)$$

with an average slope of 10.10 and average bias of -16.84. With a resolution of 0.125 mV in ADC readings, the smallest estimated current converted from the ADC is 1.26 nA.

3.3. Hardware validation

Figure 7 shows the CV response of 2.88 μM insulin measured using our custom potentiostat on one of the sensors used. The Savitzky-Golay (S-G) filter [28] was applied to smooth the CV response, with the aim to reduce noise without distorting the shape and height of the prominent peak. The principle of the S-G filter involves fitting a least squares polynomial to a set of data points defined by the window length and convolving it across the entire data. In this study, a second-order polynomial with a window length of 40 data points was employed.

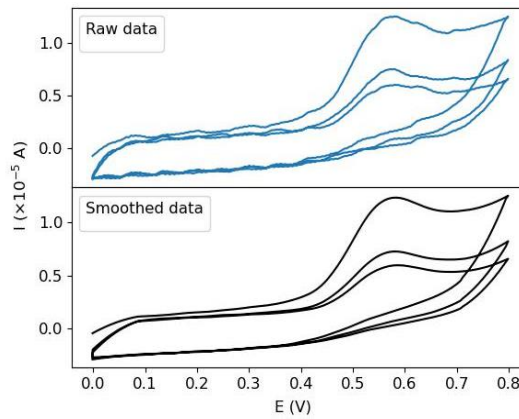


Figure 7. Raw and smoothed CV response of 2.88 μM insulin using Savitzky-Golay filter

CV measurements were performed using our custom potentiostat with the same parameters as those of the benchtop potentiostat. Figure 8(a) shows the first cycle response for each concentration, and Figure 8(b) presents the calibration curves for each cycle. The highest sensitivity was observed in the first cycle data, despite having the lowest R^2 and highest standard error among the cycles. Figure 9 compares baseline-subtracted responses for the same concentrations between the benchtop (dashed line) and our potentiostat (solid line). The shift in peak potential is likely due to sensor differences caused by cycle numbers, fouling, and changes in electrode surface properties. Nonetheless, results from our potentiostat agree with those from the benchtop device, as increased concentration correlates with increased anodic peak current.

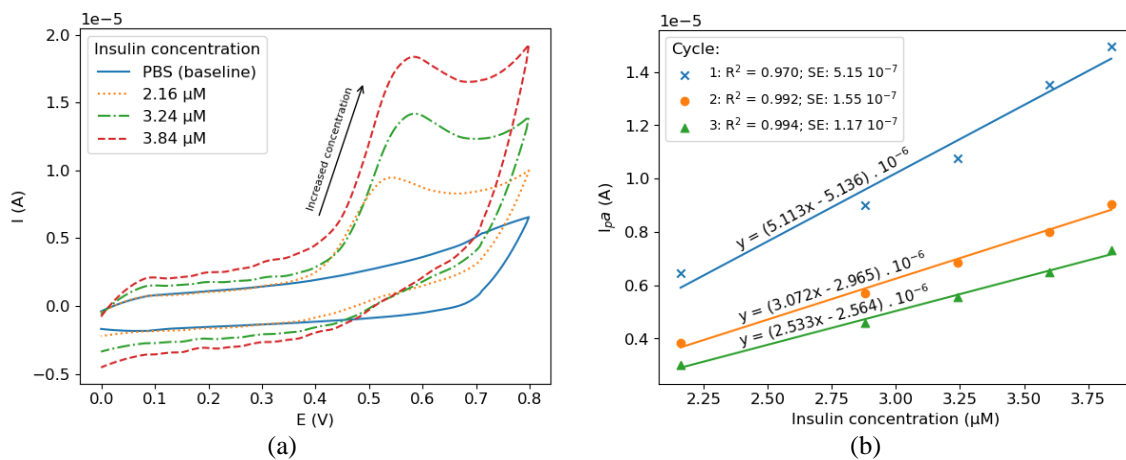


Figure 8. Peak current responses from various concentrations (a) at first cycle, and (b) all three cycles after subtracted from baseline current in the form of curve calibration

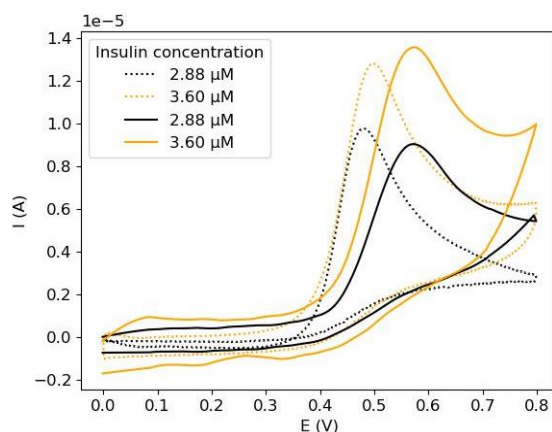


Figure 9. CV responses obtained from benchtop (dashed line) and from our potentiostat (solid line) after subtracting the baseline

3.4. Estimation system

As previously mentioned, this study proposes an estimation of insulin concentration using predictors I2, I3, and A. The fitting process to get multiple linear regression parameters was done in the training dataset. The testing dataset was then used to validate the system. There are 7 datasets obtained from 7 different sensors that were conducted with benchtop potentiostat (4 datasets: DA1, DA2, DA3, and DA4) and our potentiostat (3 datasets: DB1, DB2, DB3, and DB4). Each dataset comprises insulin concentration data with its peak currents in each 3 cycles and the sensor's electroactive area. Our proposed estimation system is basically a supervised machine learning regressor with concentration as its label, and selected predictors as its features. The R^2 score, mean squared error (MSE) and mean absolute error (MAE) were used as metrics to evaluate the estimation of the single-predictor and our proposed method as listed in Table 3.

Table 3. Performance evaluation of the estimation methods across different datasets

Predictor (s)	Data train			Data test SA4			Data test SB1			Data test SB2		
	R^2	MSE	MAE	R^2	MSE	MAE	R^2	MSE	MAE	R^2	MSE	MAE
I1	0.83	0.31	0.41	0.64	1.61	1.07	0.90	0.03	0.17	-	0.34	0.52
I2, I3, A	0.92	0.15	0.28	0.92	0.25	0.41	0.87	0.09	0.19	0.86	0.04	0.19

The first method is analogous to the single-predictor approach which uses calibration curve of peak current versus concentration. Here, the single-predictor system utilized the peak current from the first cycle (I1) to estimate the concentration. The R^2 value from the training dataset was relatively low owing to the high variance caused by different sensors, as illustrated in Figure 10. The regression parameters derived from this training data struggle to accurately estimate concentration if the dataset includes a sensor with significantly different performance. Among the three sets of test data, one exhibited a low R^2 value, one is high, and one is completely unexplainable by the trained model (negative R^2). Thus, although one sensor may yield good estimation results, this does not apply to the other two sensors, indicating that using a single predictor does not yield consistent results across all testing sensors.

The proposed method, on the other hand, demonstrated good results across all different data tests ($R^2 > 0.85$). By incorporating peak current from two cycles and the electroactive area, the system was able to generalize well to several data tests. In terms of computational complexity, although the training of our method was more complex than that of the single-predictor method, the testing process remained simple because the system only needed to compute multiplications of parameters with predictor values. The testing complexity can be expressed as $O(m)$, where m represents the number of predictors. In this scenario, our method presents no challenges for real-time applications because there is no significant difference in computation time compared to the single-predictor method.

To further validate the results, cross-validation was conducted using the dataset combinations presented in Table 4. Given that some sensors exhibited similar electroactive area values, the selected training combinations were carefully chosen to ensure significant variation in electroactive area. As shown in the table, all combinations yielded testing results with an R^2 value exceeding 0.85, demonstrating robust performance.

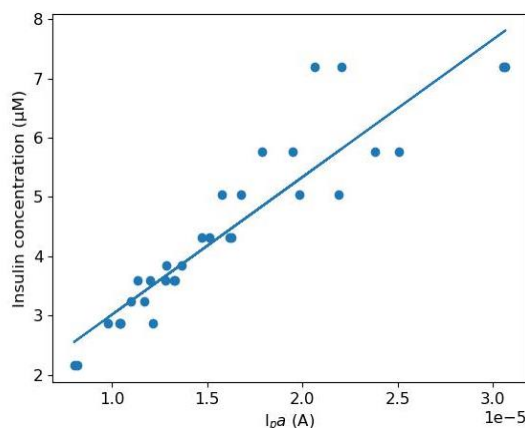


Figure 10. Estimating insulin concentration with peak current of the first cycle (I1) as predictor

Table 4. Cross validation performance in training and testing data

Training dataset	Testing dataset	Training			Testing		
		R ²	MSE	MAE	R ²	MSE	MAE
D1, D2, D3, D5	D4, D6, D7	0.92	0.17	0.29	0.90	0.35	0.45
D1, D2, D3, D6	D4, D5, D7	0.93	0.14	0.29	0.90	0.27	0.40
D1, D2, D3, D7	D4, D5, D6	0.93	0.15	0.28	0.90	0.20	0.37
D1, D2, D4, D5	D3, D6, D7	0.90	0.21	0.33	0.96	0.05	0.19
D1, D2, D4, D6	D3, D5, D7	0.93	0.16	0.31	0.88	0.23	0.34
D1, D2, D4, D7	D3, D5, D6	0.92	0.16	0.31	0.87	0.21	0.36
D1, D2, D5, D6	D3, D4, D7	0.89	0.17	0.31	0.88	0.46	0.50
D1, D2, D5, D7	D3, D4, D6	0.89	0.18	0.32	0.86	0.51	0.51
D1, D2, D6, D7	D3, D4, D5	0.91	0.15	0.29	0.89	0.39	0.47

To ensure that there was indeed a statistically significant relationship between each predictor and the concentration values, hypothesis testing was also conducted. The null hypothesis stated that the coefficient of each predictor is equal to 0, indicating that each predictor does not have a significant relationship with concentration. With a total of 75 data points and 3 predictors, the computed p-values for each predictor, I2, I3, and A, were 8.52×10^{-10} , 3.68×10^{-7} , and 0.006, respectively. All three p-values obtained were < 0.05 , thus rejecting the null hypothesis. This means that with a 95% confidence level, all predictors have a statistically significant relationship with the concentration values.

There are still not many studies reporting methods to determine concentration from CV response other than using calibration curves with single predictor. A novel analytical approach that does not rely on the typical calibration curve has been proposed by Chen and Chen [29]. In their study, they determined the concentration of pesticide using inverse calibration and high-order polynomial fitting. Their dataset had 20 replicates in each concentration with pH ranging from 6.5 to 6.8. With these many replicates, even the peak current could not serve as useful detection index for concentration. Their idea was using area from CV curve as determination variable. The comparison of the resulting R² can be seen in Table 5. They calculated R² from the fitting data, therefore we compared with the R² from training.

Table 5. Comparison of concentration estimation without conventional curve calibration

Ref.	Method	Predictor	R ²
[29]	3-order Polynomial	CV area between 0.5 and 0.9 V	0.78
[29]	3-order Polynomial	CV area between 0.5 and 1.1 V	0.86
This work	Multiple linear regression	I2, I3, and A	> 0.90

It is worth noting that the disadvantage of using electroactive area as predictor is that the necessity to re-calculate the surface area periodically due to its declining performance of sensor over time. For future research, alternative methods need to be explored that can predict the decline in surface area values based on the baseline CV shape. This approach will eliminate the need for continuous measurement of sensor surface area.

3.5. Implementation system

The use of a portable potentiostat offers a significant advantage over benchmark potentiostats: the ability to perform real-time concentration estimations. Portable potentiostats are fully customizable and can be easily connected to other devices, whereas benchtop potentiostats typically come with proprietary software designed for general electrochemical analysis. This software is often not easily configurable for specific tasks such as integration with an external API. In contrast, with our potentiostat, data migration is straightforward because the entire process can be fully customized to meet specific requirements.

The MIT App Inventor platform was used to design the mobile application due to its simplicity and ease of visually creating an app using drag-and-drop programming. Because the complex computations are handled by a computer server, the application only requires basic features. Therefore, selecting this platform is a highly efficient approach. The application includes basic UI components such as labels, buttons, BLE connections, and a web component to call the API with HTTP requests. The user interface display of our mobile application is shown in Figure 11. More details on the block diagrams of the estimation system's algorithm and implementation, as well as an explanation of the mobile app program, can be found in the Supplementary Information.

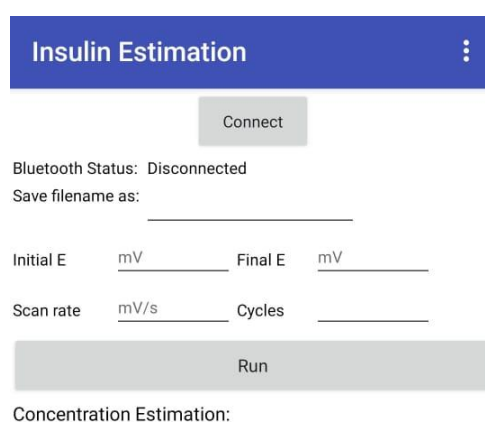


Figure 11. Graphical user interface (GUI) of our insulin estimation mobile app

4. CONCLUSION

In summary, an insulin concentration estimation device was built using a wireless, low-cost, and portable potentiostat. CV analysis responses from our potentiostat aligned well with those of the benchtop device. Despite the unavoidable noise even after filtering, our portable potentiostat effectively captured microampere-level currents. The smallest voltage it can generate is 4.4 mV and the smallest current resolution it can calculate is 1.26 nA. To ensure robust concentration estimation across sensors with varying electroactive surface areas, the proposed method utilized multiple predictors: peak currents from the second and third cycles, and electrode surface area. This approach achieved R^2 values exceeding 0.85 across all three datasets using different sensors, surpassing the performance of the single predictor method that lacked consistency across all tests. The cross validation results also yielded R^2 values more than 0.85 for all testing datasets and more than 0.90 for all training datasets. The hypothesis testing showed that the surface area as a predictor had a statistically significant relationship with concentration with a p-value of 0.006, proving that its relationship was not due to random chance. For future development, detecting even lower insulin concentrations, including analytes from those in body fluids, should be considered. Additionally, replacing the electroactive surface area as a predictor with baseline CV curve could eliminate the need for continuous electroactive area measurement, as the baseline curve characteristics may indirectly reflect the sensor's declining performance over time, ensuring more practical and efficient usability.

FUNDING INFORMATION

This research was supported by the FMIPA Postgraduate Research Grant under Grant No. PKS-043/UN2.F3.D/PPM.00.02/2024. The authors would like to express their gratitude to FMIPA Universitas Indonesia for the financial support.

AUTHOR CONTRIBUTIONS STATEMENT

All authors have read and agreed to the published version of the manuscript.

Name of Author	C	M	So	Va	Fo	I	R	D	O	E	Vi	Su	P	Fu
Fitria Yunita Dewi	✓	✓	✓	✓	✓	✓	✓	✓	✓	✓	✓		✓	
Harry Kusuma Aliwarga	✓	✓			✓	✓						✓		✓
Djati Handoko	✓	✓			✓	✓	✓	✓	✓	✓		✓	✓	✓

C : Conceptualization

M : Methodology

So : Software

Va : Validation

Fo : Formal analysis

I : Investigation

R : Resources

D : Data Curation

O : Writing - Original Draft

E : Writing - Review & Editing

Vi : Visualization

Su : Supervision

P : Project administration

Fu : Funding acquisition

CONFLICT OF INTEREST STATEMENT

Authors state no conflict of interest.

DATA AVAILABILITY

The data that support the findings of this study are available from the corresponding author DH upon reasonable request.




REFERENCES

- [1] A. Arvinte, A. C. Westermann, A. M. Sesay, and V. Virtanen, "Electrocatalytic oxidation and determination of insulin at CNT-nickel-cobalt oxide modified electrode," *Sensors and Actuators B: Chemical*, vol. 150, no. 2, pp. 756–763, Oct. 2010, doi: 10.1016/j.snb.2010.08.004.
- [2] H. Lee, Y. J. Hong, S. Baik, T. Hyeon, and D. Kim, "Enzyme-based glucose sensor: from invasive to wearable device," *Advanced Healthcare Materials*, vol. 7, no. 8, Apr. 2018, doi: 10.1002/adhm.201701150.
- [3] IDF Diabetes Atlas, "IDF Diabetes Atlas 2021 _ IDF Diabetes Atlas," Brussels, 2021.
- [4] J. Shepa *et al.*, "NiO nanoparticles for electrochemical insulin detection," *Sensors*, vol. 21, no. 15, p. 5063, Jul. 2021, doi: 10.3390/s21155063.
- [5] G. S., R. V. Siva Reddy, and M. R. Ahmed, "Personalized diabetes diagnosis using machine learning and electronic health records," *International Journal of Electrical and Computer Engineering (IJECE)*, vol. 14, no. 4, pp. 4791–4801, Aug. 2024, doi: 10.11591/ijece.v14i4.pp4791-4801.
- [6] S. D. Psoma and C. Kanthou, "Wearable insulin biosensors for diabetes management: advances and challenges," *Biosensors*, vol. 13, no. 7, p. 719, Jul. 2023, doi: 10.3390/bios13070719.
- [7] N. I. Wardani, T. Kangkamano, R. Wannapob, P. Kanatharana, P. Thavarungkul, and W. Limbut, "Electrochemical sensor based on molecularly imprinted polymer cryogel and multiwalled carbon nanotubes for direct insulin detection," *Talanta*, vol. 254, p. 124137, Mar. 2023, doi: 10.1016/j.talanta.2022.124137.
- [8] P. Businova *et al.*, "Voltammetric sensor for direct insulin detection," *Procedia Engineering*, vol. 47, pp. 1235–1238, 2012, doi: 10.1016/j.proeng.2012.09.376.
- [9] A. Noorbakhsh and A. I. K. Alnajjar, "Antifouling properties of reduced graphene oxide nanosheets for highly sensitive determination of insulin," *Microchemical Journal*, vol. 129, pp. 310–317, Nov. 2016, doi: 10.1016/j.microc.2016.06.009.
- [10] Y. Lin, L. Hu, L. Li, and K. Wang, "Facile synthesis of nickel hydroxide-graphene nanocomposites for insulin detection with enhanced electro-oxidation properties," *RSC Adv.*, vol. 4, no. 86, pp. 46208–46213, 2014, doi: 10.1039/C4RA06648K.
- [11] R. Ahmad *et al.*, "KAUSTat: a wireless, wearable, open-source potentiostat for electrochemical measurements," in *2019 IEEE SENSORS*, Oct. 2019, pp. 1–4. doi: 10.1109/SENSORS43011.2019.8956815.
- [12] A. Ainla *et al.*, "Open-source potentiostat for wireless electrochemical detection with smartphones," *Analytical Chemistry*, vol. 90, no. 10, pp. 6240–6246, May 2018, doi: 10.1021/acs.analchem.8b00850.
- [13] M. D. M. Dryden and A. R. Wheeler, "DStat: a versatile, open-source potentiostat for electroanalysis and integration," *PLOS ONE*, vol. 10, no. 10, p. e0140349, Oct. 2015, doi: 10.1371/journal.pone.0140349.
- [14] P. Lopin and K. V. Lopin, "PSoC-Stat: a single chip open source potentiostat based on a Programmable System on a Chip," *PLOS ONE*, vol. 13, no. 7, p. e0201353, Jul. 2018, doi: 10.1371/journal.pone.0201353.
- [15] A. A. Rowe *et al.*, "CheapStat: an open-source, 'Do-It-Yourself' potentiostat for analytical and educational applications," *PLoS ONE*, vol. 6, no. 9, p. e23783, Sep. 2011, doi: 10.1371/journal.pone.0023783.
- [16] P. Wu, G. Vazquez, N. Mikstas, S. Krishnan, and U. Kim, "Aquisift: A low-cost, hand-held potentiostat for point-of-use electrochemical detection of contaminants in drinking water," in *2017 IEEE Global Humanitarian Technology Conference (GHTC)*, Oct. 2017, pp. 1–4. doi: 10.1109/GHTC.2017.8239306.
- [17] I. Anshori *et al.*, "Design of smartphone-controlled low-cost potentiostat for cyclic voltammetry analysis based on ESP32 microcontroller," *Sensing and Bio-Sensing Research*, vol. 36, p. 100490, Jun. 2022, doi: 10.1016/j.sbsr.2022.100490.
- [18] A. V. Cordova-Huaman, V. R. Jauja-Ccana, and A. La Rosa-Toro, "Low-cost smartphone-controlled potentiostat based on Arduino for teaching electrochemistry fundamentals and applications," *Heliyon*, vol. 7, no. 2, p. e06259, Feb. 2021, doi: 10.1016/j.heliyon.2021.e06259.
- [19] L. H. B. Vidotto, D. Wachholz Junior, and L. T. Kubota, "A simple and low-cost portable potentiostat with real-time data sharing for wireless electrochemical analyses," *Journal of Electroanalytical Chemistry*, vol. 937, p. 117414, May 2023, doi:

- 10.1016/j.jelechem.2023.117414.
- [20] Y. C. Li *et al.*, “An easily fabricated low-cost potentiostat coupled with user-friendly software for introducing students to electrochemical reactions and electroanalytical techniques,” *Journal of Chemical Education*, vol. 95, no. 9, pp. 1658–1661, Sep. 2018, doi: 10.1021/acs.jchemed.8b00340.
- [21] M. W. Glasscott, M. D. Verber, J. R. Hall, A. D. Pendergast, C. J. McKinney, and J. E. Dick, “SweepStat: a Build-It-Yourself, two-electrode potentiostat for macroelectrode and ultramicroelectrode studies,” *Journal of Chemical Education*, vol. 97, no. 1, pp. 265–270, Jan. 2020, doi: 10.1021/acs.jchemed.9b00893.
- [22] J. L. Knopp, L. Holder-Pearson, and J. G. Chase, “Insulin units and conversion factors: a story of truth, boots, and faster half-truths,” *Journal of Diabetes Science and Technology*, vol. 13, no. 3, pp. 597–600, May 2019, doi: 10.1177/1932296818805074.
- [23] E. Martínez-Periñán *et al.*, “Insulin sensor based on nanoparticle-decorated multiwalled carbon nanotubes modified electrodes,” *Sensors and Actuators B: Chemical*, vol. 222, pp. 331–338, Jan. 2016, doi: 10.1016/j.snb.2015.08.033.
- [24] F. Y. Dewi *et al.*, “Electrochemical performance of gold nanoparticles decorated on multi-walled carbon nanotube (MWCNT) screen-printed electrode (SPE),” *ITM Web of Conferences*, vol. 61, p. 01019, Jan. 2024, doi: 10.1051/itmconf/20246101019.
- [25] B. Rafiee and A. R. Fakhari, “Electrocatalytic oxidation and determination of insulin at nickel oxide nanoparticles-multiwalled carbon nanotube modified screen printed electrode,” *Biosensors and Bioelectronics*, vol. 46, pp. 130–135, Aug. 2013, doi: 10.1016/j.bios.2013.01.037.
- [26] J. Wang and M. Musameh, “Electrochemical detection of trace insulin at carbon-nanotube-modified electrodes,” *Analytica Chimica Acta*, vol. 511, no. 1, pp. 33–36, May 2004, doi: 10.1016/j.aca.2004.01.035.
- [27] N. Elgrishi, K. J. Rountree, B. D. McCarthy, E. S. Rountree, T. T. Eisenhart, and J. L. Dempsey, “A practical beginner’s guide to cyclic voltammetry,” *Journal of Chemical Education*, vol. 95, no. 2, pp. 197–206, Feb. 2018, doi: 10.1021/acs.jchemed.7b00361.
- [28] A. Savitzky and M. J. E. Golay, “Smoothing and differentiation of data by simplified least squares procedures,” *Analytical Chemistry*, vol. 36, no. 8, pp. 1627–1639, Jul. 1964, doi: 10.1021/ac60214a047.
- [29] J. Chen and C. Chen, “A new data analysis method to determine pesticide concentrations by cyclic voltammetry,” *Measurement*, vol. 46, no. 6, pp. 1828–1833, Jul. 2013, doi: 10.1016/j.measurement.2013.02.001.

BIOGRAPHIES OF AUTHORS






Fitria Yunita Dewi    received the B.Sc. degree in physics from Universitas Indonesia, in 2019. Currently, she is a post-graduate student at the same Department with her undergraduate study. Her research interest include instrumentation, embedded-system, machine learning, and battery’s predictive maintenance. She can be contacted at email: fitria.yunita@sci.ui.ac.id.



Harry Kusuma Aliwarga    is the President Commissioner of UMG IdeaLab, an Indonesia-based corporate venture capital and co-owner of UMG Myanmar. Born and bred in Jakarta, Kiwi began his professional career in business development at Astra International and United Tractors-Indonesia from early to mid-90s before founding UMG Myanmar in 1998 with his partner MarLar Win. He holds a BSc in industrial engineering from Institut Teknologi Indonesia, a MSc in engineering from Thailand’s Asia Institute of Technology and a MSc in System Dynamics at MIT’s Sloan School of Management. He is currently completing his PhD in agriculture from Gadjah Mada University, Indonesia. He can be contacted at email: inquiry@kiwialiwarga.com.



Djati Handoko    is currently the Chairman of the Physics Department in Universitas Indonesia and actively lecturing on the Instrumentation Physics group. He received his Dr. degree from the Physics Department, Chungbuk National University, Cheongju, South Korea, whereas his BS and MS degrees in physics are from University of Indonesia. His doctorate research deals with the Magneto-Optical Kerr Effect (MOKE) and Faraday Rotation. He can be contacted at email: djati.handoko@ui.ac.id.